

## Manganese Metallamacrocycles with Various Coordination Solvents

Jiheh Song, Dohyun Moon, and Myoung Soo Lah\*

*Department of Chemistry, College of Science and Technology, Hanyang University,  
1271 Sa-1-dong, Ansan, Kyunggi-do 425-791, Korea  
Received December 18, 2001*

The hexanuclear metallamacrocycles were observed repeatedly in various conditions including the presence of several different tricationic metal ions in the macrocyclic ring system and of the linear alkyl chains at the acyl site of *N*-acylsalicylhydrazide ligand, which contrasts to the formation of the decanuclear metallamacrocycles with bulkier side chains such as phenyl group at the acyl site of the ligand. We synthesized a series of metallamacrocycles in various solvents to find the relationship between the solvents and the nuclearity of the metallamacrocycles. Whether the solvents are sterically more demanding or not, the complexes formed kept the hexanuclear metallamacrocycles system.

**Keywords:** Manganese metallamacrocycles, Hexanuclear metallamacrocycles, *N*-Acylsalicylhydrazide, Macrocyclic ring, Self-assembly.

### Introduction

Self-assembly is one of efficient methods for the synthesis of various supramolecular species.<sup>1</sup> Supramolecular architectures are comprised of both discrete molecular assembly<sup>2</sup> and inorganic crystal engineering.<sup>3</sup> The common strategy for the inorganic crystal engineering relies upon the proper programming of building units that usually made up with metal ions and spacers. The design and preparation of micro/mesoporous materials is very important because of its potential applications such as chiral separations and catalyses.<sup>4</sup> However, the drawback of this method arises from the tendency of such systems to self-intercalate, thereby reducing the accessible pore/cavity size.<sup>5</sup> When a framework with a large enough cavity was obtained, the framework is usually non-rigid and loses its structural integrity in the air.<sup>6</sup> One tactic to achieve the frameworks with large cavity and robustness is the use of large secondary building blocks.<sup>7</sup> Several research groups have synthesized and characterized inorganic clusters which could serve as secondary building units for the construction of the multi-dimensional networks with desirable properties. One way to control the cavity size and functionality of the porous frameworks could be by the modulation of the secondary building units. We recently synthesized a new type of the secondary building units, metallamacrocycles<sup>8</sup> and utilized these building units for the construction of the porous network.<sup>7c</sup> The metallamacrocycles are composed of the replaceable parts, the solvent molecules coordinated to the metal ions and non-replaceable parts, metal ions and ligands. The properties of the building units could be modulated by the change of the metal ions, ligands and solvents coordinated to the metal centers. We could introduce several tricationic octahedral metal ions such as manganese, iron, cobalt, and gallium in the metal-

lamacrocycles with their undisturbed structural features. The ligands having the various lengths of linear alkyl groups also gave the isostructural hexanuclear metallamacrocycles. However when the ligand with bulkier benzyl group was used for the synthesis of the metallamacrocycles, a decanuclear metallamacrocycles was obtained.<sup>9</sup>

In this study, we wanted to know whether it is possible to modulate the metallamacrocycles with various solvent molecules coordinated to the metal centers. We extended the solvents from methanol and dimethylformamide (dmf) to dimethylsulfoxide (dmsO), pyridine, methanol/pyridine, and dimethylacetamide (dma). The metallamacrocycles with various solvents have been characterized using X-ray crystallography and other physical methods.

### Experimental Section

**Materials.** The following were used as received with no further purification: salicylhydrazide, propionic anhydride, hexanoyl chloride and triethylamine from Aldrich, Inc.; manganese acetate tetrahydrate from Yakuri; dmsO, dma, and pyridine (py) from Carlo Erba. Pentadentate ligands, *N*-acetylsalicylhydrazide (H<sub>3</sub>ashz), *N*-propionylsalicylhydrazide (H<sub>3</sub>pshz), *N*-hexanoylsalicylhydrazide (H<sub>3</sub>hshz) and *N*-lauroylsalicylhydrazide (H<sub>3</sub>lshz) were synthesized by coupling of the salicylhydrazide and the corresponding acyl chlorides or acyl anhydrides.<sup>8b</sup>

**Physical Methods.** C, H, N and S determinations were performed by the Elemental Analysis Laboratory of the Korean Basic Science Institute. Infrared spectra were recorded as KBr pellets in the range 4000-600 cm<sup>-1</sup> on a BioRad FT-IR spectrometer. Room-temperature magnetic susceptibilities of well-ground solid samples were measured by using a Guoy method. The measurements were calibrated against a Hg[Co(SCN)<sub>4</sub>] standard.

#### Synthesis

##### Synthesis of Metallamacrocycles.

\*Corresponding Author: Phone: +82-31-400-5496, Fax: +82-31-407-3863, e-mail: mslah@hanyang.ac.kr

**[Mn<sub>6</sub>(pshz)<sub>6</sub>(dmsO)<sub>6</sub>]<sub>3</sub>·3dmsO, 1:** A 0.104 g (0.499 mmol) sample of *N*-propionylsalicylhydrazide (H<sub>3</sub>pshz) was dissolved in 20 mL of dmsO. When the ligand was dissolved completely, 0.123 g (0.502 mmol) of manganese (II) acetate tetrahydrate was added to the solution without stirring. The solution was allowed to stand for a week, whereupon dark brown rectangular crystals were obtained (0.144 g, 85.1% yield). Selected IR bands (KBr pellet, cm<sup>-1</sup>): 3451, 3063, 2956, 2929, 2860, 1602, 1560, 1509, 1466, 1440, 1405, 1369, 1323, 1247, 1170, 1148, 1110, 1035, 1016, 953, 907, 858, 756, 695, 686, 639, 594. Anal. Calcd for [Mn<sub>6</sub>(pshz)<sub>6</sub>(dmsO)<sub>6</sub>]<sub>3</sub>·3dmsO (Mn<sub>6</sub>C<sub>78</sub>H<sub>108</sub>N<sub>12</sub>O<sub>27</sub>S<sub>9</sub>) (fw = 2263.95): C, 41.38; H, 4.81; N, 7.42; S, 12.74; Mn, 14.56%. Found: C, 40.89; H, 4.56; N, 7.62; S, 12.36; Mn, 13.81%. μ<sub>eff</sub>: 11.13 μ<sub>B</sub> (4.68 μ<sub>B</sub>/metal).

**Mn<sub>6</sub>(hshz)<sub>6</sub>(dma)<sub>6</sub>, 2:** A 0.124 g (0.495 mmol) sample of *N*-hexanoylsalicylhydrazide was dissolved in 15 mL of dma, and 0.123 g (0.502 mmol) of manganese (II) acetate tetrahydrate was dissolved in 15 mL of dma in another flask. The two solutions were mixed, and the combined solution was allowed to stand for five days, whereupon dark brown rectangular crystals were obtained (0.152 g, 78.9% yield). Selected IR bands (KBr pellet, cm<sup>-1</sup>): 3476, 3057, 2956, 2929, 2857, 1622, 1601, 1558, 1510, 1466, 1440, 1404, 1373, 1323, 1255, 1189, 1169, 1145, 1109, 1036, 1023, 966, 899, 859, 753, 694, 685, 592. Anal. Calcd for Mn<sub>6</sub>(hshz)<sub>6</sub>(dma)<sub>6</sub> (Mn<sub>6</sub>C<sub>102</sub>H<sub>144</sub>N<sub>18</sub>O<sub>24</sub>) (fw = 2336.00): C, 52.45; H, 6.21; N, 10.79; Mn, 14.11%. Found: C, 52.52; H, 6.47; N, 11.05; Mn, 13.98%.

**[Mn<sub>6</sub>(ashz)<sub>6</sub>(MeOH)<sub>4</sub>(py)<sub>2</sub>]<sub>4</sub>·4MeOH, 3:** A 0.097 g (0.500 mmol) sample of *N*-acetylsalicylhydrazide was dissolved in 21 mL of methanol/pyridine (20 : 1) mixed solvent. When the ligand was dissolved completely, 0.123 g (0.50 mmol) of manganese (II) acetate tetrahydrate was added to the solution without stirring. The solution was allowed to stand for three days, whereupon dark brown rectangular crystals were obtained (0.143 g, 90.7% yield). Selected IR bands (KBr pellet, cm<sup>-1</sup>): 3433, 3067, 2925, 1602, 1561, 1507, 1466, 1443, 1406, 1381, 1339, 1322, 1245, 1214, 1171, 1148, 1109, 1069, 1035, 1006, 976, 903, 858, 757, 707, 698, 679, 643, 622, 594. Anal. Calcd for [Mn<sub>6</sub>(ashz)<sub>6</sub>(MeOH)<sub>4</sub>(py)<sub>2</sub>]<sub>4</sub>·4MeOH (Mn<sub>6</sub>C<sub>72</sub>H<sub>84</sub>N<sub>14</sub>O<sub>26</sub>) (fw = 1891.17): C, 45.73; H, 4.48; N, 10.37; Mn, 17.43%. Found: C, 45.79; H, 3.89; N, 9.97; Mn, 17.60%.

**[Mn<sub>6</sub>(hshz)<sub>6</sub>(MeOH)<sub>4</sub>(py)<sub>2</sub>]<sub>4</sub>·4MeOH, 4:** A 0.125 g (0.499 mmol) sample of *N*-hexanoylsalicylhydrazide was dissolved in 21 mL of methanol/pyridine (20 : 1) mixed solvent. When the ligand was dissolved completely, 0.123 g (0.502 mmol) of manganese (II) acetate tetrahydrate was added to the solution without stirring. The solution was allowed to stand for two days, whereupon dark brown rectangular crystals were obtained (0.150 g, 81.0% yield). Selected IR bands (KBr pellet, cm<sup>-1</sup>): 3424, 3070, 2996, 2929, 2858, 1603, 1567, 1507, 1466, 1444, 1406, 1372, 1362, 1323, 1311, 1248, 1215, 1170, 1148, 1110, 1071, 1036, 1007, 898, 859, 753, 697, 685, 641, 622, 595. Anal. Calcd for [Mn<sub>6</sub>(hshz)<sub>6</sub>(MeOH)<sub>4</sub>(py)<sub>2</sub>]<sub>4</sub>·4MeOH (Mn<sub>6</sub>C<sub>96</sub>H<sub>132</sub>-

N<sub>14</sub>O<sub>26</sub>) (fw = 2227.81): C, 51.76; H, 5.97; N, 8.80; Mn, 14.80%. Found: C, 52.18; H, 5.46; N, 8.53; Mn, 14.39%.

**[Mn<sub>6</sub>(lshz)<sub>6</sub>(py)<sub>2</sub>(MeOH)<sub>4</sub>]<sub>1</sub>·MeOH, 5:** A 0.167 g (0.499 mmol) sample of *N*-lauroylsalicylhydrazide was dissolved in 21 mL of methanol/pyridine (20 : 1) mixed solvent. When the ligand was dissolved completely, 0.123 g (0.502 mmol) of manganese (II) acetate tetrahydrate was added to the solution without stirring. The solution was allowed to stand for a week, whereupon dark brown rectangular crystals were obtained (0.11 g, 50.2% yield). Selected IR bands (KBr pellet, cm<sup>-1</sup>): 3433, 3066, 2954, 2925, 2853, 1602, 1562, 1509, 1466, 1443, 1406, 1365, 1323, 1246, 1216, 1172, 1148, 1112, 1069, 1035, 1006, 905, 858, 755, 697, 688, 642, 622, 594. Anal. Calcd for [Mn<sub>6</sub>(lshz)<sub>6</sub>(py)<sub>2</sub>(MeOH)<sub>4</sub>]<sub>1</sub>·MeOH (Mn<sub>6</sub>C<sub>129</sub>H<sub>192</sub>N<sub>14</sub>O<sub>23</sub>) (fw = 2636.65): C, 58.76; H, 7.34; N, 7.44; Mn, 12.50%. Found: C, 58.42; H, 7.16; N, 7.91; Mn, 12.80%.

**Crystallographic Data Collections and Refinements of Structures.** Crystals of 1-5 were mounted on glass fiber in random orientation. Preliminary examination and data collection were performed using a Bruker SMART CCD Detector single crystal X-Ray diffractometer using a graphite monochromated Mo K radiation (λ = 0.71073 Å) source equipped with a sealed tube X-ray source at -80 °C. Preliminary unit cell constants were determined with a set of 45 narrow frames (0.3° in ω) scans. Data sets collected consist of 1286 frames of intensity data collected with a frame width of 0.3° in ω and counting time of 25 seconds/frame at a crystal to detector distance of 5.0 cm. The double pass method of scanning was used to exclude any noise. The collected frames were integrated using an orientation matrix determined from the narrow frame scans. SMART and SAINT software packages (Bruker Analytical X-ray, Madison, WI, 1997)<sup>10</sup> were used for data collection and data integration. Analysis of the integrated data did not show any decay. Final cell constants were determined by a global refinement of 8192 reflections (θ < 25.0°). Collected data were corrected for absorbance using SADABS<sup>11</sup> based upon the Laue symmetry using equivalent reflections. Structure solution and refinement of the structure were carried out using the SHELXTL-PLUS (5.03) software package (Sheldrick, G. M., Siemens Analytical X-Ray Division, Madison, WI, 1997).<sup>12</sup> All non-hydrogen atoms were refined anisotropically; hydrogen atoms were assigned isotropic displacement coefficients U(H) = 1.2U(C) or 1.5U(C<sub>methyl</sub>), and their coordinates were allowed to ride on their respective atoms using SHELXL97.

**Complex 1.** All solvent molecules coordinated to the metal centers are disordered. Two additional solvent sites were observed and both of them were statistically disordered.

**Complex 2.** In the refinement of crystal 2, all pentyl side chains of the ligands and all of the three coordinated solvent molecules were disordered. During the least-squares refinement of crystal 2, all alkyl side chains of the ligands were restrained as an ideal geometry.

**Complex 3.** One methanol molecule coordinated to the

**Table 1.** Crystal Data and Structure Refinement

	1	2	3	4	5
Formula	C <sub>30</sub> H <sub>56</sub> Mn <sub>3</sub> N <sub>6</sub> O <sub>14.5</sub> S <sub>4.5</sub>	C <sub>17</sub> H <sub>30</sub> MnN <sub>3</sub> O <sub>4</sub>	C <sub>17.5</sub> H <sub>14</sub> Mn <sub>3</sub> N <sub>7</sub> O <sub>14.5</sub>	C <sub>18</sub> H <sub>20</sub> MnN <sub>3</sub> O <sub>4</sub>	C <sub>66.5</sub> H <sub>104</sub> Mn <sub>3</sub> N <sub>7</sub> O <sub>13.5</sub>
Formula weight	1149.99	362.05	989.62	381.31	1382.39
Crystal system	triclinic	rhombohedral	monoclinic	rhombohedral	triclinic
Space group	<i>P</i> $\bar{1}$	<i>R</i> $\bar{3}$	<i>P</i> 2 <sub>1</sub> / <i>n</i>	<i>R</i> $\bar{3}$	<i>P</i> $\bar{1}$
Unit cell dimensions	a = 10.873(2) Å b = 14.800(3) Å c = 15.846(3) Å $\alpha$ = 94.950(5) $^\circ$ $\beta$ = 103.425(4) $^\circ$ $\gamma$ = 97.137(4) $^\circ$	a = 25.277(7) Å b = 25.277(7) Å c = 15.124(5) Å $\alpha$ = 90 $^\circ$ $\beta$ = 90 $^\circ$ $\gamma$ = 120 $^\circ$	a = 15.8491(14) Å b = 10.4156(9) Å c = 27.184(2) Å $\alpha$ = 90 $^\circ$ $\beta$ = 96.007(2) $^\circ$ $\gamma$ = 90 $^\circ$	a = 27.6906(17) Å b = 27.6906(17) Å c = 12.2389(11) Å $\alpha$ = 90 $^\circ$ $\beta$ = 90 $^\circ$ $\gamma$ = 120 $^\circ$	a = 14.7657(15) Å b = 15.6372(17) Å c = 18.613(2) Å $\alpha$ = 78.065(2) $^\circ$ $\beta$ = 67.440(2) $^\circ$ $\gamma$ = 63.630(2) $^\circ$
Volume	2443.5(8) Å <sup>3</sup>	8368(4) Å <sup>3</sup>	4462.9(7) Å <sup>3</sup>	8127.1(10) Å <sup>3</sup>	3552.3(7) Å <sup>3</sup>
Z	2	18	4	18	2
Absorption coefficient	1.025 mm <sup>-1</sup>	0.736 mm <sup>-1</sup>	0.908 mm <sup>-1</sup>	0.752 mm <sup>-1</sup>	0.589 mm <sup>-1</sup>
Crystal size	0.58×0.28×0.14 mm <sup>3</sup>	0.50×0.35×0.15 mm <sup>3</sup>	0.60×0.22×0.11 mm <sup>3</sup>	0.48×0.37×0.13 mm <sup>3</sup>	0.62×0.29×0.10 mm <sup>3</sup>
$\theta$ range for data colletns	1.40 to 28.33 $^\circ$	1.61 to 28.34 $^\circ$	1.43 to 28.33 $^\circ$	1.47 to 28.26 $^\circ$	1.67 to 28.30 $^\circ$
Reflections collected	31477	16870	26726	15977	21404
Independent reflections	11492 [R(int)=0.0321]	4443 [R(int)=0.1112]	10666 [R(int)=0.0255]	4362 [R(int)=0.0473]	15701 [R(int)=0.0212]
Completeness to $\theta$	94.3%	95.3%	95.8%	97.3%	88.9%
Data/restraints params	11492 / 0 / 694	4443 / 21 / 253	10666 / 0 / 590	4362 / 0 / 281	15701 / 2 / 846
Goodness-of-fit on I <sup>2</sup>	1.045	1.183	1.392	1.138	1.056
Final R indices	R <sub>1</sub> = 0.0592, [I > 2 $\sigma$ (I)] wR <sub>2</sub> = 0.1699	R <sub>1</sub> = 0.0787, wR <sub>2</sub> = 0.1834	R <sub>1</sub> = 0.0507, wR <sub>2</sub> = 0.1410	R <sub>1</sub> = 0.0961, wR <sub>2</sub> = 0.2473	R <sub>1</sub> = 0.0659, wR <sub>2</sub> = 0.1781
R indices (all data)	R <sub>1</sub> = 0.0842, wR <sub>2</sub> = 0.1898	R <sub>1</sub> = 0.1150, wR <sub>2</sub> = 0.2085	R <sub>1</sub> = 0.0558, wR <sub>2</sub> = 0.1438	R <sub>1</sub> = 0.1276, wR <sub>2</sub> = 0.2679	R <sub>1</sub> = 0.0833, wR <sub>2</sub> = 0.1999
Largest diff. peak & hole	0.908 and -0.804 e.Å <sup>-3</sup>	0.541 and -0.461 e.Å <sup>-3</sup>	0.968 and -0.360 e.Å <sup>-3</sup>	3.059 and -0.886 e.Å <sup>-3</sup>	0.803 and -0.738 e.Å <sup>-3</sup>

$$R_1 = \frac{\sum |F_o - |F_c||}{\sum |F_o|}, \quad wR_2 = \left[ \frac{\sum w(F_o^2 - F_c^2)^2}{\sum wF_o^4} \right]^{1/2}$$

metal center was disordered. Five solvent sites were observed, and three of them were partially occupied and statistically disordered.

**Complex 4.** In the refinement of crystal 4, all of the non-hydrogen atoms except N1 atom were refined with anisotropic displacement coefficients.

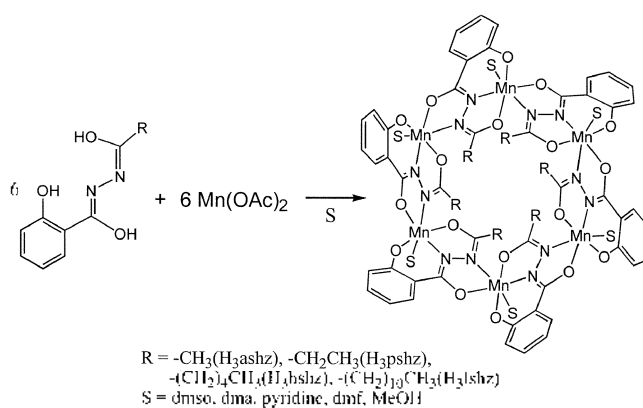
**Complex 5.** Three solvent sites were observed, and one solvent methanol located at the crystallographic inversion center was treated with disorder model.

The final residual values for the observed reflections ( $I > 2\sigma(I)$ ) and for all reflections, and relevant structure refinement parameters are listed in Table 1.

## Results and Discussion

The general reaction scheme for the preparation of metal-lamacrocycles, applicable in coordinating solvents dmf, MeOH, dmso, dma and MeOH/pyridine, is given in Scheme 1.

Regardless the solvent used all metallamacrocycles are isostructural to the previously reported 18-membered hexanuclear manganese metallamacrocycles.<sup>8b</sup> The metallamacrocycles with six metal ions are disc-shaped with different thickness depending on the ligands used. The cores of the all disc-shaped hexanuclear metallamacrocycles are approximately 2 nm in diameter and 1 nm in thickness. The

**Scheme 1**

pentadentate ligand *N*-acetylsalicylhydrazide bridges the ring metal ions using a hydrazide N-N group. An iminophenolate group and an iminoacyl group of a ligand are coordinated to the metal ion as a tridentate ligand. A hydrazide group of the other ligand occupies two of the three remaining coordination sites of the octahedral manganese (III) ion as a bidentate ligand. A various monodentate solvent molecule finishes the octahedral geometry of the tricationic metal ion.

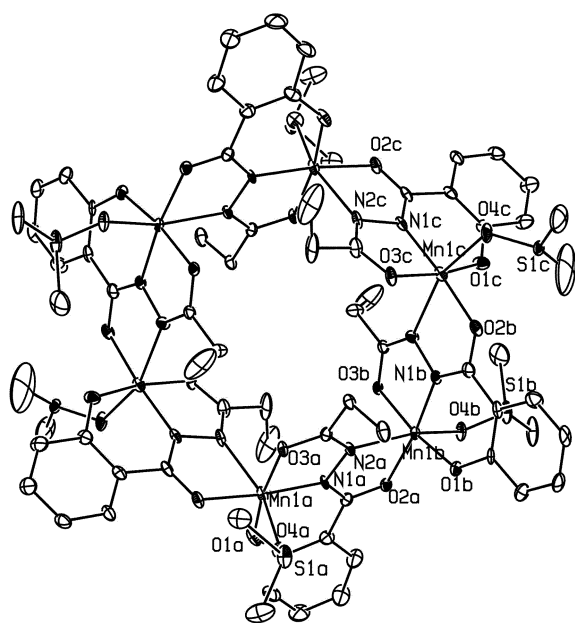


**Figure 1.** An ORTEP drawing of complex **1**,  $\text{Mn}_6(\text{pshz})_6(\text{dmsO})_6$ . The complex is in the crystallographic inversion center. A, B, and C in manganese ions could be related to each other using a noncrystallographic  $S_6$  symmetry operation. Cyclic (Mn-N-N) $_6$  linkage shows 18-membered macrocyclic ring system. The minor part of the disordered dmsO and hydrogen atoms have been omitted for clarity.

#### Crystal Structure of $[\text{Mn}_6(\text{pshz})_6(\text{dmsO})_6] \cdot 4\text{dmsO} \cdot \text{H}_2\text{O}$ ,

**1.** Hexanuclear manganese metallamacrocycle  $[\text{Mn}(\text{pshz})(\text{dmsO})_6]$ , **1** could be synthesized using manganese(II) acetate tetrahydrate as a metal source,  $\text{pshz}^{3-}$  as a trianionic pentadentate ligand and dmsO as solvent. An ORTEP diagram of **1** is shown in Figure 1. **1** with noncrystallographic local pseudo- $C_3$  symmetry is in the crystallographic inversion center. This neutral hexanuclear manganese metallamacrocycle is similar to previously reported hexanuclear manganese metallamacrocycle  $[\text{Mn}(\text{pshz})(\text{dmf})_6]$ , **8** (Table 2 and Table 3).<sup>8b</sup> A dmsO molecule is coordinated at the one end of Jahn-Teller elongation axis of the manganese(III) ions (Table 2).

**Crystal Structure of  $\text{Mn}_6(\text{hshz})_6(\text{dma})_6$ , 2.** Hexanuclear manganese metallamacrocycle  $\text{Mn}_6(\text{hshz})_6(\text{dma})_6$ , **2** could be synthesized using  $\text{hshz}^{3-}$  as a ligand and dma as solvent. An ORTEP diagram of **2** is shown in Figure 2. **2** is in the crystallographic  $C_3$  symmetry site. This neutral hexanuclear manganese metallamacrocycle is again similar to previously

**Table 2.** Bond Lengths (Å) and Angles (°) for Metallamacrocycles

	1	2	3	4	5
Mn(1A)-O(1A)	1.864	1.864(4)	1.865	1.869(4)	1.861
Mn(1A)-O(2C) <sup>d</sup>	1.974	1.980(3)	1.967	1.989(4)	1.990
Mn(1A)-O(3A)	1.933	1.929(3)	1.935	1.931(4)	1.919
Mn(1A)-N(1A)	1.940	1.945(3)	1.940	1.949(4)	1.941
Mn(1A)-O(4A)	2.203	2.188(3)	2.248	2.308(5)	2.265
Mn(1A)-N(2C) <sup>d</sup>	2.275	2.276(4)	2.244	2.267(5)	2.256
O(1A)-Mn(1A)-O(2C) <sup>d</sup>	95.5	95.3(1)	95.24	97.6(2)	97.0
O(1A)-Mn(1A)-O(3A)	170.0	170.8(1)	170.80	169.1(2)	170.5
O(1A)-Mn(1A)-O(4A)	91.9	92.0(2)	92.91	88.3(2)	89.0
O(1A)-Mn(1A)-N(1A)	90.3	90.7(2)	90.81	88.6(2)	90.8
O(1A)-Mn(1A)-N(2C) <sup>d</sup>	94.0	94.0(2)	92.54	96.7(2)	95.0
O(3A)-Mn(1A)-O(2C) <sup>d</sup>	94.4	93.9(1)	93.44	92.0(2)	92.1
O(2C) <sup>d</sup> -Mn(1A)-O(4A)	84.8	84.3(1)	85.01	84.8(2)	83.1
N(1A)-Mn(1A)-O(2C) <sup>d</sup>	173.4	173.4(1)	173.41	173.4(2)	172.1
O(2C) <sup>d</sup> -Mn(1A)-N(2C) <sup>d</sup>	74.4	74.2(1)	75.07	74.5(2)	74.5
O(3A)-Mn(1A)-O(4A)	88.9	88.7(1)	87.28	87.4(2)	89.3
O(3A)-Mn(1A)-N(1A)	79.8	80.1(1)	80.02	82.1(2)	90.2
O(3A)-Mn(1A)-N(2C) <sup>d</sup>	88.8	88.7(1)	90.42	90.9(2)	90.2
N(1A)-Mn(1A)-O(4A)	98.0	98.2(1)	94.68	97.7(2)	98.0
O(4A)-Mn(1A)-N(2C) <sup>d</sup>	158.6	158.1(1)	159.72	159.2(2)	157.3
N(1A)-Mn(1A)-N(2C) <sup>d</sup>	102.3	102.7(1)	104.72	102.7(2)	104.1

**1.**  $\text{Mn}_6(\text{pshz})_6(\text{dmsO})_6$ ; **2.**  $\text{Mn}_6(\text{hshz})_6(\text{dma})_6$ ; **3.**  $\text{Mn}_6(\text{ashz})_6(\text{MeOH})_4(\text{py})_2$ ; **4.**  $\text{Mn}_6(\text{hshz})_6(\text{py})_6$ ; **5.**  $\text{Mn}_6(\text{hshz})_6(\text{MeOH})_4(\text{py})_2$ .

<sup>d</sup>Symmetry transformation used to generate equivalent atoms.

reported hexanuclear manganese metallamacrocycle  $[\text{Mn}(\text{hshz})(\text{dmf})_6]$ , **9** (Table 2 and Table 3).<sup>8b</sup> In this complex, solvent molecule, dma, was coordinated to the metal center instead of dmf molecule.

**Crystal Structure of  $[\text{Mn}_6(\text{ashz})_6(\text{MeOH})_4(\text{py})_2] \cdot 7\text{MeOH}$ , 3.** Hexanuclear manganese metallamacrocycle  $\text{Mn}_6(\text{ashz})_6(\text{MeOH})_4(\text{py})_2$ , **3** could be synthesized using  $\text{ashz}^{3-}$  as a trianionic pentadentate ligand in MeOH/pyridine mixed solvent system (20 : 1). An ORTEP diagram of **3** is shown in Figure 3. Hexanuclear manganese metallamacrocycle **3** is also similar to previously reported hexanuclear manganese metallamacrocycle  $[\text{Mn}(\text{ashz})(\text{dmf})_6]$ , **7** except the solvent molecules coordinated to the metal centers. Methanol and pyridine molecules are coordinated to the metal center in 2 : 1 ratio even though the amount of methanol presents in excess compared to that of pyridine in solution.

**Crystal Structure of  $\text{Mn}_6(\text{hshz})_6(\text{py})_6$ , 4.** Hexanuclear

**Table 3.** Bond Lengths (Å) and Angles (°) for Metallamacrocycles

	1	2	3	4	5	6 <sup>a</sup>	7 <sup>b</sup>	8 <sup>b</sup>	9 <sup>b</sup>	10 <sup>a</sup>	11 <sup>c</sup>
Mn1A-Mn1B <sup>d</sup>	4.91	4.91	4.88	4.90	4.89	4.81	4.92	4.89	4.88	4.88	4.95
Mn1A-Mn1C <sup>e</sup>	8.20	8.19	8.22	8.21	8.28	8.03	8.21	8.26	8.18	8.27	9.27
Mn1A-Mn1B-Mn1C	113.6	113.0	115.0	114.0	115.0	111.4	114.6	115.2	113.9	115.5	138.5

**1.**  $\text{Mn}_6(\text{pshz})_6(\text{dmsO})_6$ ; **2.**  $\text{Mn}_6(\text{hshz})_6(\text{dma})_6$ ; **3.**  $\text{Mn}_6(\text{ashz})_6(\text{MeOH})_4(\text{py})_2$ ; **4.**  $\text{Mn}_6(\text{hshz})_6(\text{py})_6$ ; **5.**  $\text{Mn}_6(\text{hshz})_6(\text{MeOH})_4(\text{py})_2$ ; **6.**  $\text{Mn}_6(\text{hshz})_6(\text{MeOH})_6$ ; **7.**  $\text{Mn}_6(\text{ashz})_6(\text{dmf})_6$ ; **8.**  $\text{Mn}_6(\text{pshz})_6(\text{dmf})_6$ ; **9.**  $\text{Mn}_6(\text{hshz})_6(\text{dmf})_6$ ; **10.**  $\text{Mn}_6(\text{hshz})_6(\text{MeOH})_6$ ; **11.**  $\text{Mn}_6(\text{bzshz})_6(\text{MeOH})_6$ .

<sup>a</sup>Ref. 8a. <sup>b</sup>Ref. 8b. <sup>c</sup>Ref. 10. <sup>d</sup>Distance between non-crystallographic  $S_6$  symmetry-related atoms. <sup>e</sup>Distance between non-crystallographic  $C_3$  symmetry-related atoms.

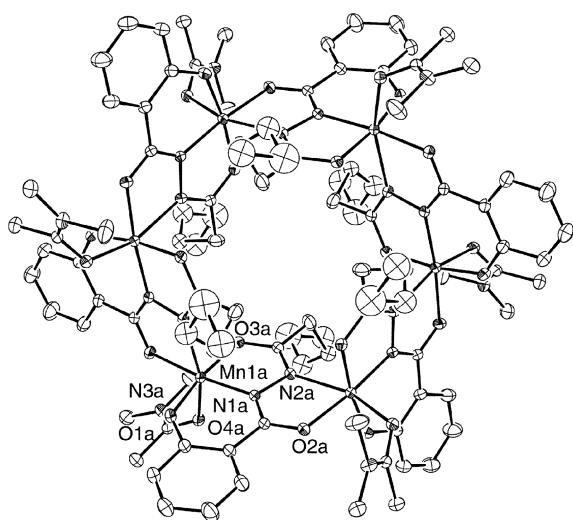


**Figure 2.** An ORTEP drawing of complex **2**,  $\text{Mn}_6(\text{hshz})_6(\text{dma})_6$ . The complex is in the crystallographic  $S_6$  symmetry site. The manganese ions could be related to each other using a crystallographic  $S_6$  symmetry operation. Hydrogen atoms have been omitted for clarity.

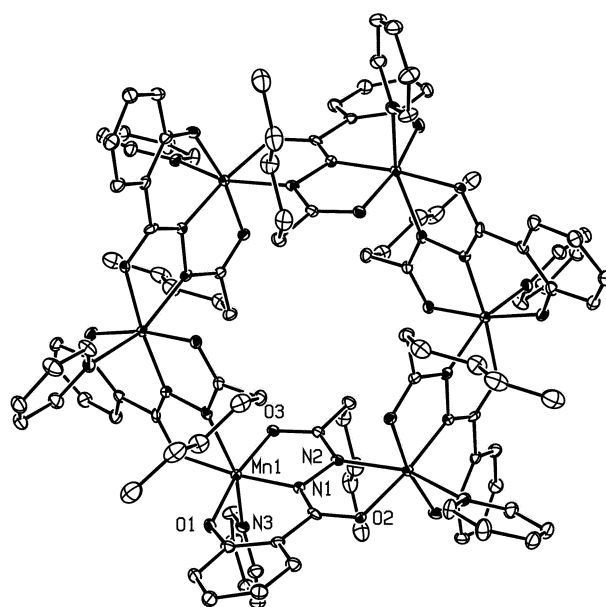


**Figure 4.** An ORTEP drawing of complex **4**,  $\text{Mn}_6(\text{hshz})_6(\text{py})_6$ . The complex is in the crystallographic  $S_6$  symmetry site. The manganese ions could be related to each other using a crystallographic  $S_6$  symmetry operation. Hydrogen atoms have been omitted for clarity.

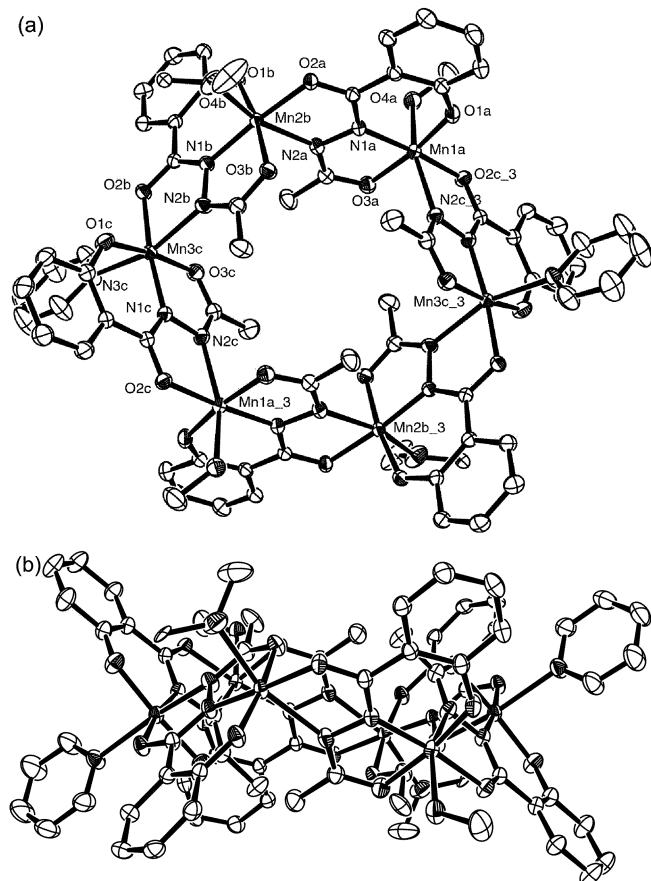


**Figure 3.** (a) An ORTEP drawing of complex **3**,  $\text{Mn}_6(\text{ashz})_6(\text{MeOH})_4(\text{py})_2$ . The complex is in the crystallographic inversion center. A, B, and C in manganese ions could be related to each other using a pseudo- $S_6$  symmetry operation. The methanol is coordinated to the manganese A center and B center, the pyridine is coordinated to the manganese C center. Hydrogen atoms have been omitted for clarity. (b) Side view of complex of complex **3** shows the thickness of the disc-shaped metallamacrocycle.

manganese metallamacrocycle  $\text{Mn}_6(\text{hshz})_6(\text{py})_6$ , **4** could be synthesized using  $\text{hshz}^{3-}$  as a trianionic pentadentate ligand again in MeOH/pyridine mixed solvent system. An ORTEP diagram of **4** is shown in Figure 4. **4** is in the crystallographic  $C_{3i}$  symmetry site. Contrast to **3**, every solvent molecule in the metal center is pyridine. No methanols were coordinated to the metal centers. However it is not clear whether all the solvent molecules in the metal centers are pyridine or the mixed solvents are coordinated to the metal centers but not observed in the crystal structure because of the disorder of the solvent molecules. Elemental analysis supports the mixed solvent coordination in the metal centers as in **3**.

**Crystal Structure of  $[\text{Mn}_6(\text{lshz})_6(\text{MeOH})_4(\text{py})_2] \cdot 5\text{MeOH}$ , **5**.** Hexanuclear manganese metallamacrocycle  $\text{Mn}_6(\text{lshz})_6(\text{MeOH})_4(\text{py})_2$ , **5** could be synthesized using  $\text{lshz}^{3-}$  as a trianionic pentadentate ligand again in MeOH/pyridine mixed solvent system. An ORTEP drawing of one of these molecules (complex **5**) is shown in Figure 5. Mixed solvent coordination of methanol and pyridine at 2 : 1 ratio was again observed as in **3**. The three alternating hydrophobic alkyl chains are aligned approximately at a right angle to the plane of the metallamacrocycle, and the other three-alkyl chains are aligned in the opposite direction as in **4**. (Figure 5b)

The hexanuclear metallamacrocycles were observed repeatedly in various conditions including the variation of the ring metals using several different tricationic metal ions and the introduction of the linear alkyl groups at the site of the acyl group of the ligand. However, the introduction of bulkier group such as phenyl group at the alkyl site of the ligand resulted in the expansion of the metallamacrocycles

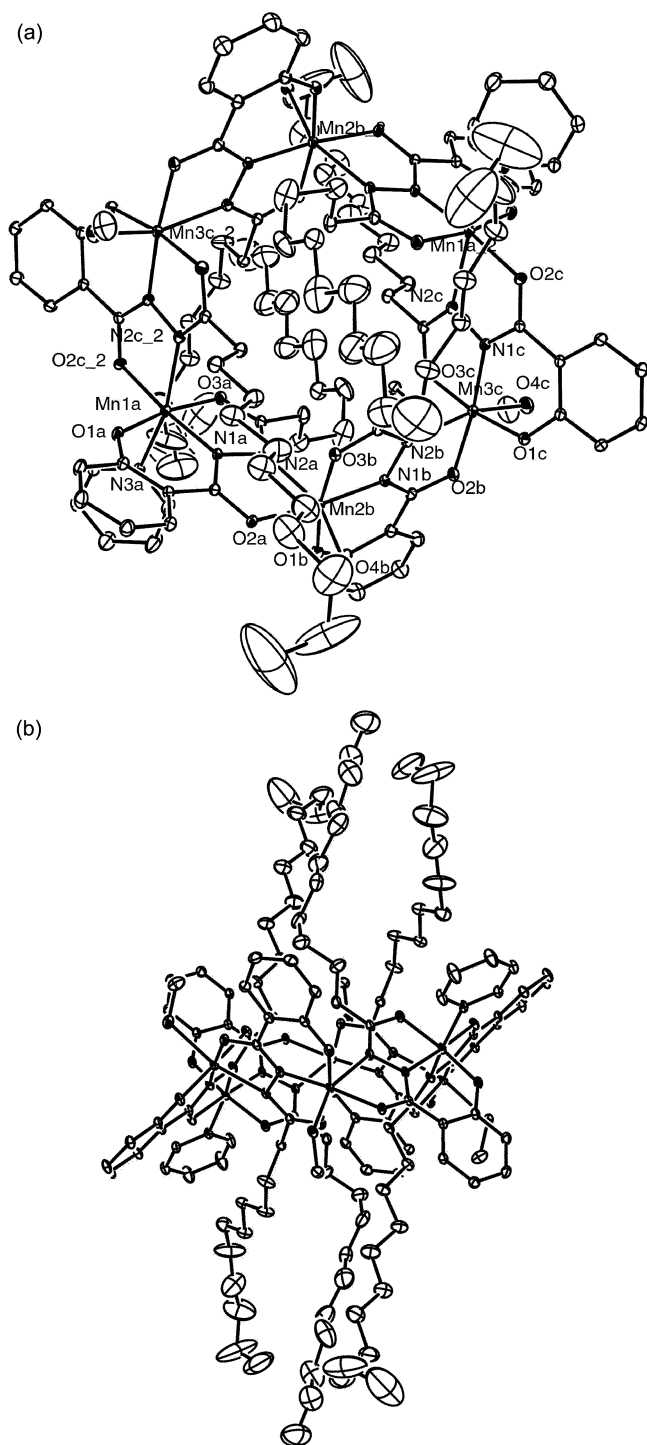


**Figure 5.** (a) An ORTEP drawing of complex **5**,  $Mn_6(lshz)_6(MeOH)_4(py)_2$ . As in complex **3**, complex **5** is in the crystallographic inversion center and A, B, and C in manganese ions could be related to each other using a pseudo- $S_6$  symmetry operation. The methanol is coordinated to the manganese B center and C center, the pyridine is coordinated to the manganese A center. Hydrogen atoms have been omitted for clarity. (b) Side view of complex **5**. The alternating side chains are aligned approximately at a right angle to the plane of the metallamacrocycle.

from hexanuclear metallamacrocycles to the decanuclear metallamacrocycle.<sup>9</sup> The phenyl group in the ligand might

cause the severe steric hindrance between those groups as in hexanuclear metallamacrocycle. To release the steric hindrance, the macrocyclic ring system of the metallamacrocycle expanded from 18-membered to 30-membered ring system (Table 3).

We could get hexanuclear metallamacrocycles with sterically less demanding solvents such as methanol and dmf. Even though more sterically demanding solvent molecules such as dmsO, dma, and pyridine were introduced at the solvent site of the metal ion of the metallamacrocycle, the resulting system still keep the 18-membered hexanuclear metallamacrocycle. Although there are some minor variations in the shapes and properties, all metallamacrocycles with various lengths of hydrophobic aliphatic linear chain and various coordination solvent molecules are isostructural 18-membered hexanuclear metallamacrocycles. Five donor atoms from two chelating pentadentate ligands and an additional donor atom from a solvent molecule have coordinated each metal center in the metallamacrocycles. The presence of these various replaceable solvents also indicates that hexanuclear metallamacrocycles could be used as nanoscale secondary building units for the preparation of porous frameworks.

**Acknowledgment.** This work was supported by the Basic Research Program of the Korea Science & Engineering Foundation (Grant No. R01-2000-000430) and Hanyang University (the program year of 2001).

**Supporting Information Available:** X-ray crystallographic files in CIF format for the structure determinations of complex **1-5** are available on request from the correspondence author.

## References

- (a) Lehn, J.-M. *Supramolecular Chemistry: Concepts and Perspectives*; VCH: New York, 1995. (b) Cram, D. J.; Cram, J. M. *Container Molecules and Their Guests*; The Royal Society of Chemistry: Cambridge, UK, 1994.
- (a) Swieggers, G. F.; Malefeste, T. J. *Chem. Rev.* **2000**, *100*, 3483-3538. (b) Caulder, D. L.; Raymond, K. N. *Acc. Chem. Res.* **1999**, *32*, 975-982. (c) Fujita, M. *Chem. Soc. Rev.* **1998**, *6*, 417-425. (d) Leininger, S.; Olcnyuk, B.; Stang, P. J. *Chem. Rev.* **2000**, *100*, 853-908. (e) Ullmer, E.; Demleitner, B.; Bernt, I.; Saalfrank, R. W. In *Structure and Bonding*; Fujita, M., Ed.; Springer: Berlin, 2000; Vol. 96, pp 149-175.
- (a) Goodgame, D. M. L.; Menzer, S.; Smith, A. M.; Williams, D. J. *J. Chem. Soc., Dalton Trans.* **1997**, 3213-3218. (b) Hirsch, K. A.; Wilson, S. C.; Moore, J. S. *Chem. Eur. J.* **1997**, *3*, 765-771. (c) Robson, R. *J. Chem. Soc., Dalton Trans.* **2000**, 3735-3744. (d) Hargman, P. J.; Hargman, D.; Zubietta, J. *Angew. Chem., Int. Ed.* **1999**, *38*, 2638-2684. (e) Braga, D.; Grepioni, F.; Desiraju, G. R. *Chem. Rev.* **1998**, *98*, 1375-1405.
- (a) Zaworotko, M. J. *Angew. Chem., Int. Ed.* **2000**, *39*, 3052-3054. (b) Yaghi, O. M.; Li, H.; Davis, C.; Richardson, D.; Groy, T. L. *Acc. Chem. Res.* **1998**, *31*, 474-484. (c) Rao, C. N. R.; Natarajan, S.; Choudhury, A.; Neeraj, S.; Ayi, A. A. *Acc. Chem. Res.* **2001**, *34*, 80-87. (d) Janiak, C. *Angew. Chem., Int. Ed.* **1997**, *36*, 1431-1434.
- (a) Batten, S. R.; Robson, R. *Angew. Chem., Int. Ed.* **1998**, *37*, 1460-1494. (b) Biradha, K.; Domasevitch, K. V.; Moulton, B.; Seward, C.; Zaworotko, M. J. *Chem. Commun.* **1999**, 1327-1328.

- (c) Barnett, S. A.; Blake, A. J.; Champness, N. R.; Nicolson, J. E. B.; Wilson, C. *J. Chem. Soc., Dalton Trans.* **2001**, 567-573. (d) Gardner, G. B.; Venkataraman, D.; Moore, J. S.; Lee, S. *Nature* **1995**, *374*, 792-795. (e) Kondo, M.; Yoshitomi, T.; Seki, K.; Matsuzaka, H.; Kitagawa, S. *Angew. Chem., Int. Ed.* **1997**, *36*, 1725-1727.
6. (a) Prior, T. J.; Rosseinsky, M. *J. Chem. Commun.* **2001**, 495-496. (b) Biradha, K.; Fujita, M. *Chem. Commun.* **2001**, 15-16.
7. (a) Yaghi, O. M.; Li, H.; Davis, C.; Richardson, D.; Groy, T. L. *Acc. Chem. Res.* **1998**, *31*, 474-484. (b) Kim, J.; Chen, B.; Reineke, T. M.; Li, H.; Eddaoudi, M.; Moler, D. B.; O'Keefe, M.; Yaghi, O. M. *J. Am. Chem. Soc.* **2001**, *129*, 8239-8247. (c) Moon, M.; Kim, I.; Lah, M. S. *Inorg. Chem.* **2000**, *39*, 2710-2711. (d) Lee, E.; Kim, J.; Heo, J.; Whang, D.; Kim, K. *Angew. Chem., Int. Ed.* **2001**, *40*, 399-402.
8. (a) Kwak, B.; Rhee, H.; Park, S.; Lah, M. S. *Inorg. Chem.* **1998**, *37*, 3599-3602. (b) Kwak, B.; Rhee, H.; Lah, M. S. *Polyhedron* **2000**, *19*, 1985-1994. (c) Kwak, B.; Kim, I.; Lah, M. S. *Inorg. Chim. Acta* **2001**, *317*, 12-20.
9. Liu, S.-X.; Lin, S.; Lin, B.-Z.; Lin, C.-C.; Huang, J.-Q. *Angew. Chem., Int. Ed.* **2001**, *40*, 1084-1087.
10. SMART and SAINT, Area Detector Software Package and S.A.Y. Area detector Integration Program. Bruker Analytical X-ray; Madison, WI, 1997.
11. SADABS, Area Detector Absorption Correction Program; Bruker Analytical X-ray; Madison, WI, 1997.
12. Sheldrick, G. M.. SHELXTL-PLUS, Crystal Structure Analysis Package; Bruker Analytical X-ray; Madison, WI, 1997.
-